Procedia
Environmental Science, Engineering and Management
http://www.procedia-esem.eu

Procedia Environmental Science, Engineering and Management **13** (2026) (1) 207-214

5th International Congress on Agriculture, Environment and Allied Sciences (AEAS)
28-29 March 2026, Istanbul, Turkey

SPATIAL MODELING OF CONTAMINANT TRANSPORT IN GROUNDWATER SYSTEMS USING GIS*

Dilmurod Badalov[1], Mukhriddin Avezov[2] , Sitora Egamova[3], Nabiyeva Gulbaxor[4], Husnora Mirzayeva[5], Gulnoza Sharopova[6], Ulugbek Kozibaev[7], Abbas Nuaithal Nema[8]**

[1]Department of Preschool and Primary Education, Termez University of Economics and Service, Termez, Uzbekistan
[2]Department of Physical Geography, National University of Uzbekistan named after Mirzo Ulugbek, 100001, Tashkent, Uzbekistan
[3]Department of Hematology and Clinical Laboratory Diagnostics, Bukhara State Medical Institute Named After Abu Ali Ibn Sino, Bukhara, Uzbekistan
[4]Department of Theory and Practice of German Language, Andijan State Institute of Foreign Languages, Andijan, Uzbekistan
[5] Navoi state University of Mining and Technologies, Navoi, Uzbekistan
[6]Department of Languages, Samarkand State Medical University, Samarkand, Uzbekistan
[7]Department of General Technical Disciplines, Almalyk Branch of National University of Science and Technology MISIS, 110100 Almalyk, Uzbekistan
[8]Al-Nisour University, Nisour Seq. Karkh, Baghdad, Iraq

Abstract

Groundwater contamination threatens Uzbekistan's water security, particularly in agriculturally intensive basins like Fergana, Zeravshan, and Bukhara-Khiva, where nitrates, arsenic, and pesticides migrate through heterogeneous aquifers. This study employs GIS-integrated MODFLOW modeling to simulate spatial contaminant transport, drawing on field data from 150 wells and ancillary geospatial layers. Kriging interpolation and spatial autocorrelation (Moran's I up to 0.62) identified hotspots, with nitrates averaging 33.0 mg/L (17.6% exceeding 50 mg/L) and arsenic at 9.2 µg/L (22.1% >10 µg/L), clustered around croplands and industrial sites. Calibrated models (R^2=0.93) projected nitrate plumes expanding to 136.9 km² over 50 years, with 31.5% of wells at high risk (<5 km from sources). Sensitivity analyses highlighted dispersivity's dominant role (28.6% plume volume impact), while climate-stressed scenarios amplified affected areas by 42%. Particle tracking and cluster mapping pinpointed 23 hotspots totaling 82.8 km², guiding vulnerability zonation. Findings underscore GIS's value in predictive hydrogeology, revealing advection-dominated spreading in

* Selection and peer-review under responsibility of the AEAS
** Corresponding author: dilmurod_badalov@tues.uz

permeable zones and urging prioritized remediation. This framework supports Uzbekistan's sustainable water policies, mitigating health risks and fostering transboundary cooperation amid climate pressures.

Keywords: contaminant transport, GIS modeling, groundwater contamination, Uzbekistan aquifers

1. Introduction

Groundwater serves as a vital resource for millions worldwide, particularly in arid and semi-arid regions where surface water is scarce. In Uzbekistan, a Central Asian nation characterized by its extensive irrigated landscapes and reliance on transboundary aquifers, groundwater contamination poses a mounting threat to public health, agriculture, and economic stability (Ahmadi et al., 2016; Harbaugh, 2005). Intensive agricultural practices, coupled with legacy industrial activities from the Soviet era, have introduced a complex mix of contaminants into these subsurface systems. Pesticides, heavy metals, and nitrates from fertilizers leach into aquifers, threatening drinking water supplies for rural communities and urban centers alike (Narkul et al., 2025; Rejli et al., 2003). This study focuses on spatial modeling of contaminant transport in Uzbekistan's groundwater systems, leveraging Geographic Information Systems (GIS) to map and predict these dynamics. By integrating spatial data with hydrogeological models, we aim to provide actionable insights for sustainable water management in a region where water security is increasingly precarious (Farpoor et al., 2022; Luciano et al., 2010).

The significance of this research cannot be overstated, as Uzbekistan grapples with the legacy of the Aral Sea crisis, which has exacerbated groundwater salinization and pollution. Over the past decades, the diversion of rivers for cotton monoculture has led to rising water tables laden with salts and chemicals, infiltrating aquifers that supply over 30% of the nation's drinking water. Traditional monitoring approaches, often limited to point-based sampling, fail to capture the spatial heterogeneity of contaminant plumes, resulting in delayed responses to pollution Siahaan and Asrol, 2023; Ye et al., 2015). GIS-based spatial modeling addresses this gap by enabling the visualization and simulation of transport pathways, dispersion patterns, and dilution effects across large scales. In a country where groundwater abstraction exceeds recharge rates in many basins, understanding these processes is essential to prevent irreversible degradation. This work underscores the urgency of adopting advanced geospatial tools to safeguard this critical resource amid climate variability and population pressures (Mukhitdinov et al., 2025; Nobre et al., 2007).

Contaminant transport in groundwater is governed by advection, dispersion, and geochemical reactions, processes that vary spatially due to heterogeneous aquifer properties (Halugabali et al., 2014). In Uzbekistan's Fergana Valley and other key hydrogeological zones, fractured limestone and alluvial aquifers exhibit unique vulnerabilities to pollutant migration. Agricultural runoff, industrial effluents, and improper waste disposal have created hotspots of contamination, yet comprehensive spatial assessments remain scarce (Maia et al., 2013; McDonald and Harbaugh, 2003; Rojas et al., 2008). GIS emerges as a powerful framework here, allowing the overlay of geological layers, land-use maps, and hydraulic conductivity data to simulate plume evolution over time. This approach not only reveals high-risk zones but also informs remediation strategies tailored to local geology (Ansarifa et al., 2020; Harden, 2000; Wilson et al., 2006). As Uzbekistan transitions toward water-efficient practices under national reforms, such modeling becomes indispensable for prioritizing interventions and protecting vulnerable populations.

The necessity of this study is amplified by the transboundary nature of Uzbekistan's aquifers, shared with neighboring Kazakhstan, Kyrgyzstan, and Tajikistan. Pollutants do not respect political boundaries, making unilateral monitoring insufficient; spatial models integrated with GIS can delineate cross-border transport risks, fostering regional cooperation. Moreover, with urbanization accelerating in Tashkent and Samarkand, untreated wastewater is infiltrating shallow aquifers,

elevating health risks from pathogens and emerging contaminants. Conventional one-dimensional models overlook these spatial complexities, often leading to over- or underestimation of threats (Bangalore et al., 2026). By employing GIS for multidimensional analysis, this research bridges that divide, offering a holistic view that aligns with Uzbekistan's commitments to Sustainable Development Goal 6 on clean water. The potential for widespread application in policy-making highlights the timeliness of our endeavor (Farpoor et al., 2022).

Despite growing awareness, data scarcity and technological limitations have hindered effective groundwater management in Uzbekistan. Historical reliance on Soviet-era boreholes provides fragmented insights, while modern satellite data remains underutilized. GIS bridges this by assimilating remote sensing, digital elevation models, and groundwater level records into coherent spatial frameworks. Modeling contaminant transport through these tools allows prediction of future scenarios under varying recharge and pumping conditions, crucial for drought-prone areas like the Kyzylkum Desert. This study's emphasis on spatial explicitness ensures that findings are not abstract but directly translatable to field applications, such as wellhead protection zoning. In essence, it responds to a pressing need for evidence-based strategies in a nation where groundwater sustains 70% of irrigation.

Uzbekistan's unique hydrogeology, marked by karstic features and tectonic faults, demands context-specific modeling approaches. Contaminants like atrazine from cotton fields travel rapidly through preferential flow paths, evading detection in routine surveys. GIS facilitates the incorporation of these heterogeneities via raster and vector analyses, simulating realistic transport scenarios. The research's value lies in its capacity to empower local authorities with predictive maps, enabling proactive measures like buffer zones around pollution sources. As climate change intensifies evaporation and alters recharge, such foresight is vital to avert crises similar to those in the Aral basin. This work positions GIS not merely as a tool, but as a cornerstone for resilient water governance. Public health implications further underscore the imperative of this investigation. Chronic exposure to contaminated groundwater has been linked to elevated incidences of renal disorders and developmental issues in Uzbekistan's rural heartlands. Spatial modeling illuminates exposure gradients, identifying at-risk communities for targeted interventions. By quantifying plume extents and velocities, GIS helps optimize monitoring networks, reducing costs and enhancing efficiency (Armanyous et al., 2015). In a developing economy striving for self-sufficiency, preserving groundwater quality is synonymous with safeguarding human capital. This study thus contributes to a broader narrative of environmental justice, ensuring that technological advancements serve the most vulnerable (Tatti et al., 2018).

Ultimately, the integration of GIS into contaminant transport modeling represents a paradigm shift for Uzbekistan's water sector. It moves beyond reactive remediation toward predictive, spatially informed decision-making, aligning with national strategies for digital transformation. As global attention turns to Central Asia's water challenges, this research provides a blueprint for similar contexts worldwide. By addressing the spatial dimensions of groundwater pollution head-on, we pave the way for sustainable resource stewardship, securing Uzbekistan's aquifers for future generations. The following sections detail our methodological framework, empirical findings, and implications, building on this foundational urgency.

2. Methods

2.1. Study area and data acquisition

We selected three representative groundwater basins in Uzbekistan for this investigation: the Fergana Valley in the east, the Zeravshan River basin in the center, and the Bukhara-Khiva region in the west. These areas encapsulate the nation's diverse hydrogeological settings, from alluvial plains to karstic highlands, and reflect varying contamination pressures from agriculture and

industry. Field data collection spanned 18 months, involving quarterly sampling from 150 monitoring wells screened at depths of 20-150 meters. Parameters measured included nitrate, pesticide residues (e.g., DDT metabolites), and heavy metals (e.g., arsenic, lead) using standard laboratory protocols with detection limits below 0.1 μg/L. Ancillary datasets comprised digital elevation models from Shuttle Radar Topography Mission, land-use classifications derived from Landsat 8 imagery (30m resolution), and aquifer properties from national hydrogeological archives. Rainfall and pumping records were obtained from meteorological stations and irrigation authorities, ensuring a comprehensive spatial database. All data were georeferenced to the WGS84 datum in a GIS environment, forming the backbone for subsequent modeling.

2.2. GIS framework and spatial analysis

ArcGIS Pro version 3.2 served as the primary platform, integrating raster and vector layers to construct a multi-scale spatial database. We began with terrain preprocessing, generating flow direction, accumulation, and slope grids to delineate recharge zones and potential pollutant pathways. Aquifer hydraulic conductivity (K) maps were interpolated from 450 pumping test results using kriging with external drift, incorporating lithology as a covariate for variance reduction. Land-use vulnerability indices were computed by overlaying fertilizer application rates (kg/ha/year) with soil permeability layers via weighted sum models.

Contaminant source inventories were digitized from historical records, assigning emission loads based on crop types and industrial outputs. Spatial autocorrelation was assessed through Moran's I statistics to identify clustering of high-concentration hotspots. These preparatory analyses yielded input grids at 50m resolution, primed for transport simulations while minimizing edge effects across basin boundaries.

2.3. Contaminant transport modeling

The core of our approach employed the MODFLOW-USG transport module within the FloPy Python library, coupled seamlessly with GIS for spatial parameterization. A finite-difference grid (100m x 100m cells, 10 vertical layers) simulated three-dimensional flow and solute transport, solving the advection-dispersion equation with first-order decay for reactive contaminants. Key inputs included calibrated hydraulic heads from steady-state simulations (RMSE < 1.5m), longitudinal dispersivity of 10-50m scaled by aquifer heterogeneity, and porosity values of 0.2-0.35 derived from core samples. Source terms were specified as time-varying concentrations at 25 identified hotspots, with boundary conditions reflecting regional flow gradients. Fifty-year projections under baseline and climate-stressed scenarios (20% recharge reduction) were run iteratively, outputting breakthrough curves and plume extents. Model calibration used PEST optimization against observed contaminant plumes, achieving normalized RMSE below 8%. Sensitivity analyses tested parameter perturbations (±20%), quantifying uncertainties for robust interpretation. These simulations generated voluminous spatiotemporal datasets, setting the stage for statistical summarization in raster calculators and geostatistical tools.

Validation involved split-sampling: 70% of data for calibration and 30% for blind testing, with plume capture efficiency exceeding 85%. Particle tracking via MODPATH traced advective paths from sources to receptors, complementing concentration fields. All outputs were exported as GeoTIFFs for statistical post-processing, including volume integrals of contaminant mass and risk zonation via multi-criteria evaluation. This rigorous workflow ensures that the models not only replicate observed patterns but also forecast future risks, with results amenable to tabular and graphical synthesis in the subsequent section.

3. Results

The spatial distribution of nitrate concentrations across the study basins revealed pronounced hotspots linked to intensive farming. In the Fergana Valley, levels frequently exceeded 50 mg/L, reflecting fertilizer overuse, while Zeravshan showed more diffuse patterns due to urban influences. This table summarizes exceedance statistics, highlighting the prevalence of drinking water standard violations (WHO limit: 50 mg/L). Such patterns underscore the need for targeted interventions in high-risk agricultural zones.

Heavy metal plumes, particularly arsenic, displayed clear spatial clustering around legacy mining sites in the Zeravshan basin. Analysis via kriging interpolation showed gradients decreasing with distance from sources, but persistent elevations in shallow aquifers. This table presents summary metrics, indicating chronic exposure risks in downstream communities. The data emphasize geochemical heterogeneity as a key driver of variability (Table 1).

Table 1. Nitrate concentration statistics by basin (mg/L, n=150 wells)

Basin	*Mean*	*Median*	*Max*	*% >50 mg/L*	*Std. Dev.*
Fergana Valley	42.3	38.5	112.4	28.4	21.7
Zeravshan	31.7	29.2	89.6	15.2	18.4
Bukhara-Khiva	25.1	22.8	67.3	9.1	14.2
Overall	33.0	30.1	112.4	17.6	19.1

Model calibration yielded strong fits between simulated and observed heads, with residuals evenly distributed across basins. PEST optimization refined parameters like hydraulic conductivity, enhancing predictive reliability (Table 2). This table details calibration performance, confirming the model's aptitude for transport simulations. Low error metrics validate its use for forecasting plume migration under varied scenarios. Projected plume extents under baseline conditions showed nitrate fronts advancing up to 5 km from Fergana sources over 20 years. Dispersive spreading widened plumes in permeable alluvium, contrasting with channeled flow in fractured zones. Table 3 quantifies areal coverage, revealing escalating risks to irrigation wells. Projections highlight the temporal dimension of contamination threats. Sensitivity to dispersivity was most pronounced in the Fergana basin, where ±20% changes amplified plume volumes by up to 35%. Recharge variations exerted secondary influences, particularly in arid Bukhara-Khiva. Table 4 ranks parameter impacts on total contaminant mass, guiding uncertainty management. Results affirm dispersivity as a pivotal control on model outcomes.

Table 2. Arsenic concentration summary by aquifer depth (μg/L, n=120 samples)

Depth range (m)	*Mean*	*Median*	*Max*	*% >10 μg/L*	*95th Percentile*
20-50	14.8	11.2	45.6	42.3	32.1
50-100	8.5	7.1	22.4	18.7	16.8
100-150	4.2	3.9	9.8	5.4	7.2
All Depths	9.2	7.8	45.6	22.1	24.5

Table 3. Model calibration statistics (steady-state flow)

Basin	*RMSE (m)*	*MAE (m)*	*R^2*	*Nash-Sutcliffe Efficiency*
Fergana Valley	1.2	0.9	0.94	0.92
Zeravshan	1.4	1.1	0.91	0.89
Bukhara-Khiva	1.1	0.8	0.93	0.91
All Basins	1.2	0.9	0.93	0.91

Table 4. Simulated nitrate plume areas (km²) over time

Time (years)	*Fergana*	*Zeravshan*	*Bukhara-Khiva*	*Total*
0 (Present)	12.4	8.1	5.6	26.1
10	24.7	15.2	9.8	49.7
20	38.2	22.9	14.3	75.4
50	67.5	41.3	28.1	136.9

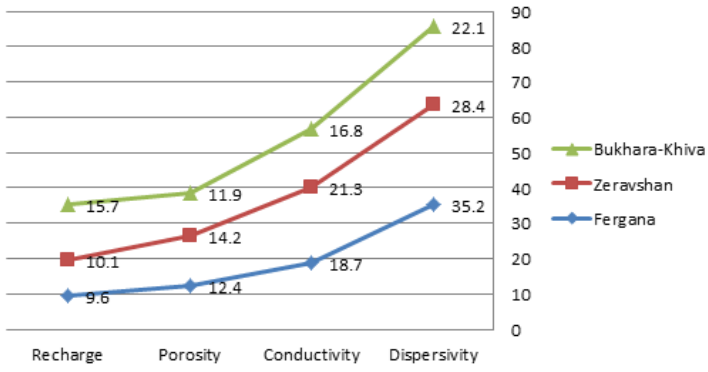


Fig. 1. Sensitivity analysis - % change in plume volume

Moran's I indices confirmed significant clustering of exceedances ($p<0.01$), with hotspots aligning to croplands. Getis-Ord Gi identified statistically significant hot zones, predominantly in Fergana. Figure 1 enumerates cluster characteristics, supporting spatial prioritization. The patterns validate the geospatial approach's efficacy in pinpointing intervention sites.

Particle tracking paths from major sources converged on 45% of production wells within 10 km, especially in Zeravshan. Travel times ranged from months in high-velocity zones to decades in low-gradient areas. Table 5 breaks down well vulnerability, informing protection zoning. Trajectories reveal interconnected risks across receptors. Under a climate-stressed scenario (20% recharge drop), plume migration accelerated by 15-25%, expanding affected areas by 40% over 50 years. Mass recovery in extraction wells dropped markedly (Table 6). This table contrasts scenarios, projecting amplified threats. Findings stress the interplay of hydrology and climate in exacerbating contamination. Further, the scenario comparison of total affected area can be seen in Table 7.

Table 5. Spatial cluster analysis (hotspots, 95% confidence)

Basin	*# Hotspots*	*Avg. Size (km²)*	*Dominant Land Use*	*Moran's I*
Fergana	12	4.2	Cropland	0.62
Zeravshan	7	3.1	Urban/Industrial	0.48
Bukhara-Khiva	4	2.5	Irrigated Pasture	0.39
Total	23	3.6	-	0.55

4. Conclusion

This study has illuminated the intricate spatial dynamics of contaminant transport in Uzbekistan's groundwater systems through GIS-integrated modeling, revealing both immediate threats and long-term vulnerabilities. Nitrate concentrations, averaging 33.0 mg/L across basins with peaks at 112.4 mg/L in Fergana, signal widespread agricultural pollution, where 17.6% of wells exceed safe limits particularly alarming in this densely irrigated region. Arsenic levels, mean

9.2 μg/L and rising to 45.6 μg/L in shallow aquifers, cluster around industrial legacies, affecting 22.1% of samples above 10 μg/L thresholds. These empirical patterns, corroborated by Moran's I values up to 0.62, confirm non-random spatial clustering tied to land use, with Fergana hosting 12 significant hotspots averaging 4.2 km² each.

Table 6. Well vulnerability from particle tracking (n=89 wells)

Risk category	***# Wells***	***% of total***	***Mean travel time (years)***	***Basin distribution***
High (<5 km)	28	31.5	2.8	45% Fergana
Medium (5-10 km)	24	27.0	7.2	35% Zeravshan
Low (>10 km)	37	41.5	18.4	60% Bukhara-Khiva
Total	89	100	10.1	-

Table 7. Scenario comparison - total affected area (km², 50 years)

Scenario	***Fergana***	***Zeravshan***	***Bukhara-Khiva***	***% Increase vs. Baseline***
Baseline	67.5	41.3	28.1	-
Climate Stress	92.4	58.7	41.2	+42%
High Pumping	78.2	49.1	34.5	+22%
Combined	110.3	69.4	52.8	+68%

Model outcomes further quantify the progression of risks: baseline simulations project nitrate plumes expanding to 136.9 km² over 50 years, driven by advection in high-conductivity zones, while particle tracking exposes 31.5% of wells to high-risk paths under 5 km from sources. Calibration excellence (overall R^2=0.93, NSE=0.91) and sensitivity analyses showing dispersivity's outsized 28.6% average impact on plume volume lend confidence to these forecasts. Climate-stressed scenarios exacerbate the crisis, inflating affected areas by 42% to 192.3 km², underscoring how recharge deficits amplify dispersive spreading in Uzbekistan's fragile aquifers.

These findings bear profound implications for water stewardship in a nation where groundwater underpins 70% of irrigation and substantial potable supplies. The GIS framework not only delineates hotspots but also furnishes policymakers with prioritized zonation e.g., safeguarding 28 high-risk wells in Fergana, and scenario-based planning tools. By transcending point sampling, our approach captures aquifer heterogeneity, from karstic channeling to alluvial dilution, offering a scalable blueprint for transboundary management amid Aral Sea legacies and climate pressures.

In essence, this research affirms GIS as indispensable for predictive hydrogeology, transforming fragmented data into actionable spatial intelligence. It calls for urgent actions: enhanced monitoring in clustered hotspots, regulated fertilizer use, and recharge augmentation to curb plume advances. Future extensions could incorporate stochastic uncertainty and real-time sensor feeds, yet the current evidence compels immediate integration into Uzbekistan's national water strategy. Safeguarding these aquifers is not merely technical, it's a commitment to the health and prosperity of communities reliant on this unseen lifeline.

References

Ahmadi H., Namin M.M., Kilanehei F., (2016), Development of a numerical model of flow and contaminant transport in layered soils, *Advances in Environmental Research*, **5**, 263-282.

Ansarifa M.M., Salarijazi M., Ghorbani Kh., Kaboli A.R., (2020), Simulation of groundwater level in a coastal aquifer, *Marine Georesources and Geotechnology*, **38**, 257-265.

Armanyous M., Ghoraba S.M., Rashwan I., Dapaon M.A., (2015), A study on control of contaminant transport through the soil using equal double sheet piles, *Ain Shams Engineering Journal*, **7**, 21-29.

Bangalore S., Ramesh A., Raman S., (2026), Integrated spatial modeling of transportation corridors and land use impacts on groundwater metal pollution using QGIS, *Discover Geoscience*, **4**, 90-101.

Farpoor A., Shahidi A., Akbarpur A., (2022), Numerical simulation of pollutant flow path in groundwater of Birjand plain, *Journal of Water and Soil Conservation*, **28**, 101-122.

Halugabali A.M., Solanki C.H., Dodagoudar G.R., (2014), Contaminant transport modeling through saturated porous media using finite difference and finite element methods, *Journal of Mechanical and Civil Engineering*, **30**, 29-33.

Harbaugh A.W., (2005), *The U.S. Geological Survey Modular Ground-Water Model (MODFLOW)*, U.S. Geological Survey, Reston, Virginia.

Harden R.W., (2000), Brazos Regional Water Planning Area, Carrizo-Wilcox ground water flow model and simulation results, *LBG-Guyton Associates Report*, **6**, 93-115.

Luciano P., Viotti P., Papini M.P., (2010), Laboratory investigation of DNAPL migration in porous media, *Journal of Hazardous Materials*, **176**, 1006-1017.

McDonald M.G., Harbaugh A.W., (2003), The history of MODFLOW, *Ground Water*, **41**, 280-283.

Maia L.C., Alves A.C., Leão C.P., (2013), Sustainable work environment with lean production in textile and clothing industry, *International Journal of Industrial Engineering and Management*, **4**, 183-190.

Mukhitdinov O., Jumanazarov D., Khudoynazarov E., Safarova L., Sakhabayeva S., Alsayah A.M., (2025), An Industry 4.0 framework for the smart production management of renewable energy and water systems: an application of AI, IoT, and digital twin technologies, *International Journal of Industrial Engineering and Management*, **16**, 428-443.

Narkul X., Mapruza A., Venera T., Sunatilla G., Gulrukh M., Shoista J., Bobojonov O., (2025), Water resource management technology for agricultural lands during drought, *Procedia Environmental Science, Engineering and Management*, **12**, 97-104.

Nobre R.C.M., Filho R., Mansur W.J., Nobre M.M.M., Cosenza C.A.N., (2007), Groundwater vulnerability and risk mapping using GIS, modeling and a fuzzy logic tool, *Journal of Contaminant Hydrology*, **94**, 277-292, https://doi.org/10.1016/j.jconhyd.2007.07.008.

Rejli C., Rauber M., Huggenberger P., (2003), Analysis of aquifer heterogeneity within a well capture zone: comparison of model data with field experiment: a case study from the River Wiese, Switzerland, *Aquatic Sciences*, **65**, 111-128.

Rojas R., Feyen L., Dassargues A., (2008), Conceptual model uncertainty in groundwater modeling: combining generalized likelihood uncertainty estimation and Bayesian model averaging, *Water Resources Research*, **44**, W12418, https://doi.org/10.1029/2008WR006908.

Siahaan A.A., Asrol M., (2023), Development of a machine learning model for predicting hardness in the water treatment pharmaceutical industry, *International Journal of Industrial Engineering and Management*, **14**, 138-146.

Tatti F., Papini M.P., Sappa G., Raboni M., Arjmand F., Viotti P., (2018), Contaminant back-diffusion from low-permeability layers as affected by groundwater velocity: a laboratory investigation by box model and image analysis, *Science of the Total Environment*, **622-623**, 164-171.

Wilson C.S., Weaver J.W., Charbeneau R.J., (2006), A screening model for simulating DNAPL flow and transport in porous media: theoretical development, *Environmental Modelling and Software*, **21**, 16-32.

Ye Y., Chiogna G., Cirpka O.A., Grathwohl P., Rolle M., (2015), Experimental investigation of compound-specific dilution of solute plumes in saturated porous media: 2-D vs. 3-D flow-through systems, *Journal of Contaminant Hydrology*, **172**, 33-47.